

Banned

An X-Ray Method for Measuring the Thickness of Thin Crystalline Films

A. EISENSTEIN

TECHNICAL REPORT No. 17

Reprinted from JOURNAL OF APPLIED PHYSICS, Vol. 17, No. 11, pp. 874-878, November, 1946

where

N = number of unit cells per unit volume or $1/V_c$ where V_c is the unit cell volume,
 p = multiplicity,
 F = crystal structure factor,
 r = camera radius, and
 $A(\theta)$ = correction for absorption in the sample.
 e , m , and c have their usual significance.

The power dP_i' diffracted from the volume element dV_i is,

$$dP_i' = KN_i^2 p_i F_i^2 (\text{L.P.})_i A(\theta) dV_i, \quad (2)$$

where

$$K = (I_0 s e^4 \lambda^3) \div (16 \pi r m^2 c^4), \quad (3)$$

and includes those terms which are independent of the particular volume element chosen. (L.P.) designates the usual Lorentz-Polarization factor.

The geometrical arrangement for the general case of diffraction from a double layer flat sample is shown in Fig. 2. A primary beam of intensity I_0 and cross section A_0 falls on the sample at an incident angle α irradiating a projected area A . This gives rise to a diffracted power dP_1' from the volume element dV_1 of layer 1 and to dP_2' from a similar volume element of layer 2. Radiation scattered from dV_1 must traverse a total path length in layer 1 of xy_1 where

$$xy_1 = x \left(\frac{1}{\sin \alpha} + \frac{1}{\sin (2\theta_1 - \alpha)} \right). \quad (4)$$

Introducing the absorption correction and

$$dV_1 = A dx, \quad (5)$$

$$dP_1' = KAN_1^2 p_1 F_1^2 (\text{L.P.})_1 \exp \{-\mu_1 xy_1\} dx, \quad (6)$$

where μ_1 is the linear absorption coefficient and F_1 the crystal structure factor for the material of this layer. By integration between the limits 0 and l , the power scattered from layer 1 of thickness l ,

$$P_1' = KAN_1^2 p_1 F_1^2 (\text{L.P.})_1 \frac{(1 - \exp \{-\mu_1 ly_1\})}{\mu_1 y_1}. \quad (7)$$

Consider the scattering from the volume element dV_2 of layer 2 which is located at a depth greater than l below the surface. The total path traversed by the diffracted rays is

$$ly_2 + xy_2 \quad (8)$$

in layers 1 and 2, respectively. By substitution

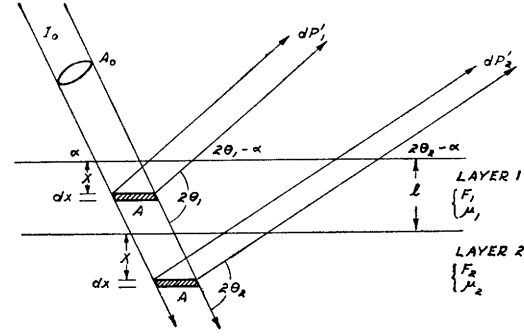


FIG. 2. Diffraction from double layer flat sample.

in (2) the diffracted power is,

$$dP_2' = KAN_2^2 p_2 F_2^2 (\text{L.P.})_2 \exp \{-\mu_1 ly_2\} \exp \{-\mu_2 xy_2\} dx. \quad (9)$$

If the absorption coefficient μ_2 is made large, either by a suitable choice of backing material or primary beam wave-length, layer 2 may be considered as having an infinite thickness for purposes of integration. Hence, integration between the limits 0 and ∞ yields,

$$P_2' = KAN_2^2 p_2 F_2^2 (\text{L.P.})_2 \frac{\exp \{-\mu_1 ly_2\}}{\mu_2 y_2}. \quad (10)$$

The ratio of integrated intensities from the materials of layers 1 and 2 is (7)/(10) or

$$\frac{P_1'}{P_2'} = \frac{N_1^2 p_1 F_1^2 \mu_2 y_2 (\text{L.P.})_1}{N_2^2 p_2 F_2^2 \mu_1 y_1 (\text{L.P.})_2} \frac{1 - \exp \{-\mu_1 ly_1\}}{\exp \{-\mu_1 ly_2\}}. \quad (11)$$

When it is convenient to select for comparison, diffraction lines from the two materials falling at approximately the same angular position, the ratio (11) may be simplified. If $\theta_1 = \theta_2$, then $y_1 = y_2$ and $(\text{L.P.})_1 = (\text{L.P.})_2$ and

$$l = \frac{1}{\mu_1 y} \ln \left\{ \frac{P_1' N_2^2 p_2 F_2^2 \mu_1}{P_2' N_1^2 p_1 F_1^2 \mu_2} + 1 \right\}. \quad (12)$$

The thickness of the surface material may thus be determined from measurements of the integrated intensities of selected diffraction lines from the two layers. A knowledge is also required of the unit cell sizes and the linear absorption coefficients of the two materials as well as the crystal structure factors and multiplicities for the particular hkl reflections.

If the materials of layers 1 and 2 have approximately the same N , p , F , and μ values, the

An X-Ray Method for Measuring the Thickness of Thin Crystalline Films

A. EISENSTEIN*

Radiation Laboratory,** Massachusetts Institute of Technology, Cambridge, Massachusetts

(Received May 31, 1946)

When x-rays are scattered from a thin crystalline surface film overlying a crystalline base material, diffraction lines are observed from both materials. Equations are developed for the general case of (1) a flat sample and (2) a cylindrical sample expressing the ratio of line intensities from the two materials as a function of film thickness. A usable range of 10^{-6} cm to 5×10^{-2} cm is indicated. Experimental confirmation is found in the range 10^{-4} cm to 6×10^{-3} cm.

INTRODUCTION

ALTHOUGH electron diffraction methods are generally used to detect and analyze thin surface films, x-ray diffraction patterns have been obtained¹ from electrodeposited films of copper as thin as 5×10^{-6} cm. In these experiments determinations of thickness were made from the time and current flow conditions of the electrodeposition process rather than from the x-ray patterns which served only to indicate the crystal structure present. Since diffraction patterns of thin surface films are composed of diffraction lines from both the underlying base material and surface layer, it seems reasonable to expect that a comparison of the relative, integrated intensities of the two sets of diffraction lines can be used as a measure of the surface film thickness. Such a comparison must take into account differences in absorption, crystal structure, and structure factor of the two materials as well as geometrical considerations. Equations are developed for use in obtaining the thickness of thin surface films on either flat or cylindrical samples. An experimental verification is found in the case of the cylindrical sample.

Since the completion of this work two abstracts have appeared describing thickness measurements of thin coatings using x-ray techniques. One of these methods,² based essentially on absorption, compares the intensities of certain diffraction lines of the base material

observed before and after coating with the surface layer. From this measured intensity ratio, the absorption coefficient of the surface material and the geometry of the arrangement, it was possible to determine metal plating thicknesses in the range 10^{-5} cm to 10^{-2} cm. The second method,³ essentially that which is described in this paper, compares the intensities of diffraction lines from the surface and base materials. An equation is shown for the special geometrical condition of back reflection and is verified experimentally in the thickness range of 10^{-4} cm.

FLAT SAMPLE

Figure 1 shows a collimated, homogeneous, primary beam of wave-length λ and intensity I_0 falling upon a mass of crystalline powder having a total volume V . A total power P is diffracted into the Debye-Scherrer halo forming a cone of semi-apex angle 2θ . The power which is diffracted into a circular segment of length s and is recorded by a cylindrical strip of film is given by⁴

$$P' = \frac{I_0 s e^4 \lambda^3}{16 \pi r m^2 c^4} N^2 V \rho F^2 \frac{1 + \cos^2 2\theta}{\sin 2\theta \sin \theta} A(\theta), \quad (1)$$

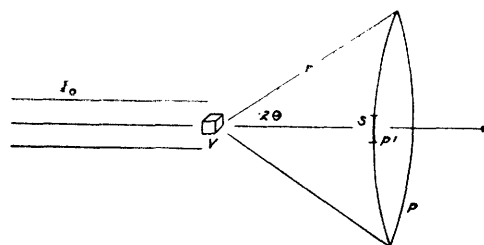


FIG. 1. Debye-Scherrer scattering from volume V .

* Now at the Physics Department, Massachusetts Institute of Technology.

** This paper is based on work done for the Office of Scientific Research and Development under contract OEMsr-262 with Massachusetts Institute of Technology.

¹ G. L. Clark, G. Pish, and L. E. Weeg, J. App. Phys. 15, 193 (1944).

² L. S. Birks and H. Friedman, Bull. Am. Phys. Soc. 20, No. 4 (1945).

³ R. B. Gray, Bull. Am. Phys. Soc. 20, No. 5 (1945).

⁴ International Tables for the Determination of Crystal Structures (Gebrüder Borntraeger, Berlin, 1935), p. 561.

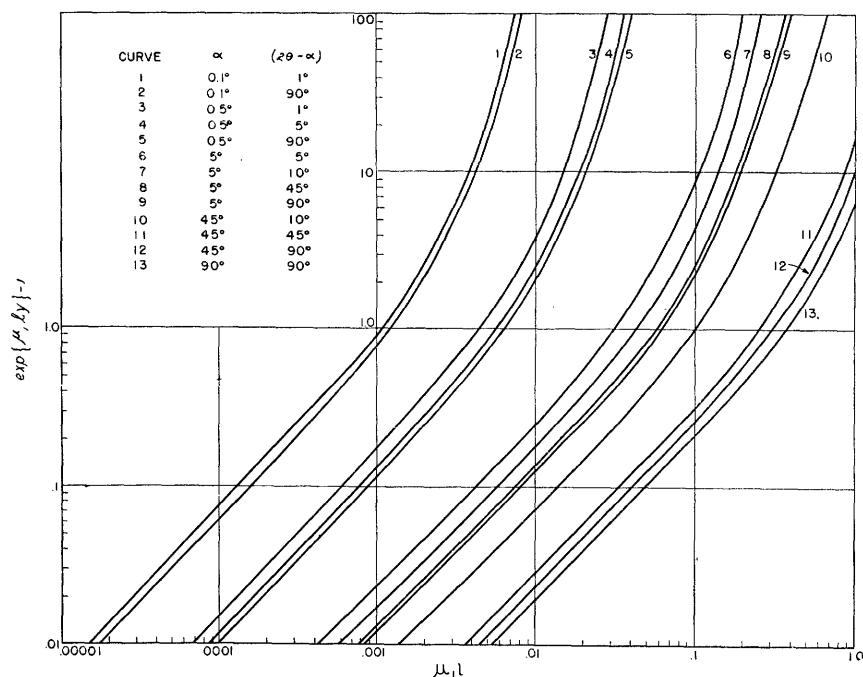


FIG. 3. $(\exp \mu_1 l y - 1)$ vs. $\mu_1 l$, see text.

ratio of diffracted powers P_1'/P_2' is simply $(\exp \{\mu_1 l y\} - 1)$. A plot of this exponential function vs. $\mu_1 l$ is shown in Fig. 3 for various values of the incidence angle α and the reflection angle $(2\theta - \alpha)$. Because of the interchangeability of α and $(2\theta - \alpha)$ in this function, these curves cover the experimental range from glancing incident angle, 0.1° , to normal incidence angle, 90° , as used in the back reflection x-ray method. In general, the variation of the exponential function with the reflection angle $(2\theta - \alpha)$ is small for a given incidence angle α , hence the diffraction lines selected for comparison need only fall in the same general angular range. Assuming the ratio P_1'/P_2' can be measured between 0.01 and 100, the experimental limits of thickness measurements by this method are seen to depend critically upon the α and $(2\theta - \alpha)$ values selected.

As an example of the application of this method, consider the simple case of a surface layer which has the same crystal structure as that of the underlying material but different lattice constant, atomic structure factor f , and absorption coefficient, e.g., silver over copper. Selecting the 400 line of Ag and the 222 line of Cu which fall at about the same angular position,

$2\theta = 95^\circ$, Table I shows values to be substituted in (12). Atomic structure values as well as linear absorption coefficients are given for the radiation wave-length of $\text{CuK}\alpha$, 1.54\AA . Assuming the ratio P_1'/P_2' measurable between 0.01 and 100, a substitution of these values into (12) leads to a measurable thickness range for glancing incidence, $\alpha = 0.5^\circ$, of 10^{-7} cm to $2 \times 10^{-5}\text{ cm}$ and for back reflection, $\alpha = 90^\circ$, of 10^{-6} cm to $2 \times 10^{-4}\text{ cm}$. The lower limit of thickness measurement could be extended, in the case of glancing incidence, by the selection of lines falling at a smaller value of 2θ , e.g., 111 of Cu and 200 of Ag. Irregularities in the surface will tend, however, to increase the practical lower limits of measurement.

CYLINDRICAL SAMPLE

Figure 4 shows a cylindrical sample of radius R and length L intercepting a primary beam of collimated radiation and scattering a diffracted

TABLE I.

	N	p	f	$F = 4f$	μ
Ag (400)	$1/(4.01)^3$	6	24.8	99.2	2280
Cu (222)	$1/(3.61)^3$	8	13.7	54.8	455

beam at an angle 2θ with the incident direction. When the absorption coefficient of either layer is large, only the surface areas AB and $A'B'$ contribute to the diffracted beam. The total diffracted power P'_{Tk} , falling in the segment s of Fig. 1, can be represented as the summation of scattering dP'_k from flat surface elements dA integrated over the effective scattering surface AB . Then,

$$P'_{Tk} = \int_A^B dP'_k, \quad (13)$$

where dP'_k is obtained by substituting dA for A in (7) or (10). Since the surface element

$$dA = LRd\alpha, \quad (14)$$

substitution into (13) yields,

$$P'_{T1} = \frac{KLRN_1^2 p_1 F_1^2 (\text{L.P.})_1}{\mu_1} \times \int_0^{2\theta_1} \frac{1 - \exp \{-\mu_1 l y_1\}}{y_1} d\alpha, \quad (15)$$

and

$$P'_{T2} = \frac{KLRN_2^2 p_2 F_2^2 (\text{L.P.})_2}{\mu_2} \times \int_0^{2\theta_2} \frac{\exp \{-\mu_1 l y_2\}}{y_2} d\alpha; \quad (16)$$

and the ratio (15)/(16),

$$\frac{P'_{T1}}{P'_{T2}} = \frac{N_1^2 p_1 F_1^2 \mu_2 (\text{L.P.})_1}{N_2^2 p_2 F_2^2 \mu_1 (\text{L.P.})_2} \times \frac{\int_0^{2\theta_1} \frac{1 - \exp \{-\mu_1 l y_1\}}{y_1} d\alpha}{\int_0^{2\theta_2} \frac{1 - \exp \{-\mu_1 l y_2\}}{y_2} d\alpha}. \quad (17)$$

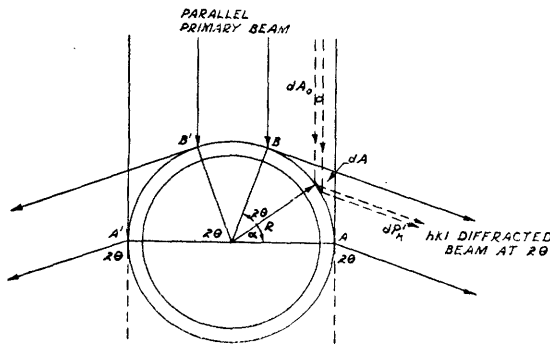


FIG. 4. Diffraction from double layer cylindrical sample.

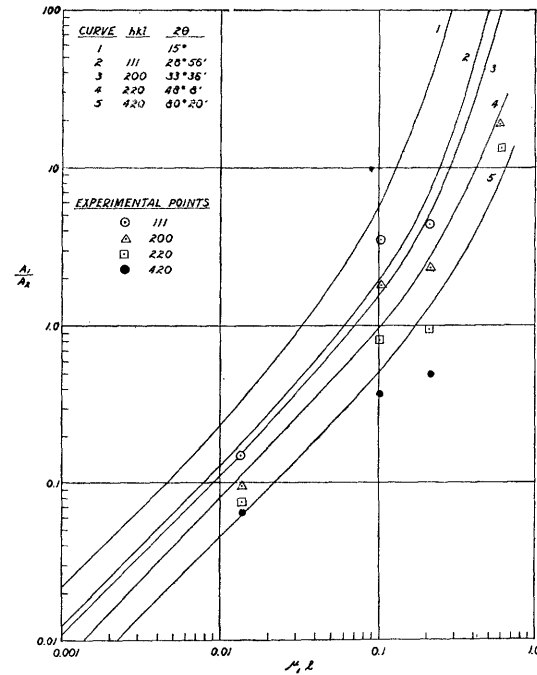


FIG. 5. Ratio of integrals of (15) and (16), A_1/A_2 , respectively, vs. $\mu_1 l$.

TABLE II.

hkl	111	200	220	420
2θ	28°51'	33°36'	48°8'	80°20'

The integrals of (15) and (16) have been solved only by graphical integration and these values are designated as A_1 and A_2 , respectively.

Selecting again for comparison, lines in the same angular range $\theta_1 = \theta_2$, then $y_1 = y_2$ and $(\text{L.P.})_1 = (\text{L.P.})_2$, hence

$$\frac{A_1}{A_2} = \frac{P'_{T1} N_2^2 p_2 F_2^2 \mu_1}{P'_{T2} N_1^2 p_1 F_1^2 \mu_2}. \quad (18)$$

The ratio A_1/A_2 was evaluated as a function of $\mu_1 l$ for specific values of 2θ . The exact values selected were 15° and those which correspond to the angular positions of diffraction lines from a (BaSr)O equal molar solid solution for Cu $K\alpha$ radiation, see Table II. The ratio A_1/A_2 is shown as a function of $\mu_1 l$ in Fig. 5. This set of curves for the case of a cylindrical sample, are seen to correspond roughly to the set in Fig. 2 for a flat sample set at an incident, glancing angle of 5° .

In practice, the ratio A_1/A_2 is obtained by means of (18) from the experimentally measured, integrated intensity ratio P'_{T1}/P'_{T2} and the thickness l determined from Fig. 5. As an example, consider again the case of an Ag layer covering a Cu base structure and compare the diffracted 400 and 222 lines, respectively. Assuming the ratio P'_{T1}/P'_{T2} can be measured between 0.01 and 100, substitution into (18) indicates a measurable thickness range of 3×10^{-6} cm to 10^{-3} cm. The selection of diffraction lines occurring at smaller 2θ positions would decrease the limits of this range, as indicated in Fig. 5.

An inspection of (7) and (10) shows that the diffracted power dP'_k per unit area dA of periphery is symmetrical with respect to variations in α , about $\alpha = \theta$. Hence, there is an asymmetrical distribution of intensity, power per unit area of diffracted beam, across the beam as it is intercepted by the film. This effect is of interest in assigning an appropriate correction for the angular displacement of diffraction lines and has been discussed^{5,6} in this connection.

EXPERIMENTAL

A series of cylindrical thickness standards were prepared to establish experimentally the validity of Eq. (18). The samples used were in the form of indirectly heated oxide cathodes. Nickel cylinders 3 mm in diameter were sprayed with a coating of BaCO_3 , sufficiently thick to prevent scattering from the underlying base metal. Over these were sprayed thin, uniform coatings of SrCO_3 of differing weights. By heating in vacuum at an uncorrected pyrometer temperature of 800°C , the carbonates were converted to the oxides BaO and SrO . At this temperature no interdiffusion of the two layers to form a solid solution could be detected in the

x-ray patterns of the wax protected cathodes.⁷ These patterns were obtained using filtered $\text{Cu } K\alpha$ radiation, a 3×0.5 -mm slit collimator and a 4.70-cm radius camera. Microphotometer tracings were made of the lines diffracted from the 111, 200, 220, and 420 planes of SrO and BaO . As both materials have the same crystal structure and differed by only 15 percent in lattice constant, the hkl lines of SrO were compared directly with the corresponding lines of BaO which fell in approximately the same angular range. The ratio P'_{T1}/P'_{T2} was simply the ratio of maximum line intensities I_1/I_2 since the shape of all diffraction lines appeared to be the same. From the spray conditions, the apparent density of the BaCO_3 and SrCO_3 layers was known to be 1.2 ± 0.2 g/cm³ and 0.8 ± 0.2 g/cm³, respectively. SrO coating thicknesses were computed from the apparent SrCO_3 density, the weight of each coating, and the coated area. These were found to be 1.3×10^{-4} cm, 1.0×10^{-3} cm, 2.0×10^{-3} cm, and 6.3×10^{-3} cm. No correction was made for the small reduction in thickness and increase in density produced in both layers during the conversion process. The experimental points, obtained from (18) with $p_1 = p_2$ and appropriate N , F , and μ values, for the oxides using the apparent density values, fall on the $A1/A2$ curves as indicated in Fig. 5.

This method of measuring film thickness has been used to determine, (1) the thickness of electrodeposited layers, (2) the extent of surface oxidation after the exposure of the sample to an oxidizing atmosphere, (3) the thickness of sprayed oxide coatings, and (4) the thickness of surface layers produced by a chemical reaction.

The author is indebted to Professor B. E. Warren for his very helpful criticism of this manuscript as well as to Miss Eleanor Uhl for the evaluation of the function presented in Fig. 5.

⁵ A. Taylor and H. Sinclair, Proc. Phys. Soc. **57**, 108 (1945).

⁶ B. E. Warren, J. App. Phys. **16**, 614 (1945).

⁷ A. Eisenstein, J. App. Phys. **17**, 434 (1946).
